Formation of a Bis(histidyl) Heme Iron Complex in Manganese Peroxidase at High pH and Restoration of the Native Enzyme Structure by Calcium †

ARTICLE *in* BIOCHEMISTRY · SEPTEMBER 2000

Impact Factor: 3.02 · DOI: 10.1021/bi000679j · Source: PubMed

4 AUTHORS, INCLUDING:

Heather Youngs
University of California, Berkeley
29 PUBLICATIONS **1,753** CITATIONS
SEE PROFILE

Pierre Moënne-Loccoz
Oregon Health and Science University
109 PUBLICATIONS **3,196** CITATIONS
SEE PROFILE

Michael H Gold
Tennessee Clinical Research Center
269 PUBLICATIONS **11,939** CITATIONS
SEE PROFILE

Formation of a Bis(histidyl) Heme Iron Complex in Manganese Peroxidase at High pH and Restoration of the Native Enzyme Structure by Calcium†

Heather L. Youngs, Pierre Moënne-Loccoz, Thomas M. Loehr, and Michael H. Gold*

Department of Biochemistry and Molecular Biology, Oregon Graduate Institute of Science and Technology, Beaverton, Oregon 97006-8921

Received March 24, 2000

ABSTRACT: Manganese peroxidase (MnP) from *Phanerochaete chrysosporium* undergoes a pH-dependent conformational change evidenced by changes in the electronic absorption spectrum. This high- to low-spin alkaline transition occurs at ∼2 pH units lower in an F190I mutant MnP when compared to the wild-type enzyme. Herein, we provide evidence that these spectral changes are attributable to the formation of a bis(histidyl) heme iron complex in both proteins at high pH. The resonance Raman (RR) spectra of both ferric proteins at high pH are similar, indicating similar heme environments in both proteins, and resemble that of ferric cytochrome b_{558}, a protein that contains a bis-His iron complex. Upon reduction with dithionite at high pH, the visible spectra of both the wild-type and F190I MnP exhibit absorption maxima at 429, 529, and 558 nm, resembling the absorption spectrum of ferrous cytochrome b_{558}. RR spectra of the reduced wild-type and F190I mutant proteins at high pH are also similar to the RR spectrum of ferrous cytochrome b_{558}, further suggesting that the alkaline low-spin species is a bis(histidyl) heme derivative. No shift in the low-frequency RR bands was observed in 75% ^{18}O-labeled water, indicating that the low-spin species is most likely not a hydroxo-heme derivative. Electronic and RR spectra also indicate that addition of Ca^{2+} to either the ferric or ferrous enzymes at high pH completely restores the high-spin pentacoordinate species. Other divalent metals, such as Mn^{2+}, Mg^{2+}, Zn^{2+}, or Cd^{2+}, do not restore the enzyme under the conditions studied.

Manganese peroxidase (MnP)[1] is an extracellular heme protein produced by virtually all lignin-degrading white-rot fungi (*1*−*3*). Sequences have been determined for *mnp* cDNA (*4*, *5*) and genomic clones (*6*−*8*) encoding three MnP isozymes from *Phanerochaete chrysosporium*, the best-studied lignin-degrading fungus. These sequences and spectroscopic studies of the native and oxidized enzyme intermediates indicate that the heme environment of MnP is similar to that of other plant and fungal peroxidases (*4*, *9*−*14*). Kinetic and spectroscopic studies of the purified enzyme indicate a typical peroxidase reaction catalytic cycle:

$$MnP + H_2O_2 \rightarrow MnPI + H_2O \quad (1)$$

$$MnPI + Mn^{2+} \rightarrow MnPII + Mn^{3+} \quad (2)$$

$$MnPII + Mn^{2+} \rightarrow MnP + Mn^{3+} + H_2O \quad (3)$$

However, MnP is unique in its ability to efficiently oxidize Mn^{2+} to Mn^{3+} (*9*, *15*, *16*). The released Mn^{3+} is stabilized by organic acid chelators, such as oxalate and malonate, which are secreted by the fungus (*16*, *17*). The Mn^{3+}-chelator complex is capable of diffusing from the enzyme to oxidize terminal substrates including lignin substructures, phenolic compounds, and pollutants (*2*, *3* and references therein, *18*).

The three amino acid residues believed to bind Mn^{2+}, D179, E35, and E39, were investigated by site-directed mutagenesis of recombinant MnP homologously expressed in *P. chrysosporium* (*19*−*22*). These studies, combined with X-ray crystal structure analyses of the proteins (*23*, *24*), confirmed that the side-chain carboxylates of D179, E35, and E39 form the only apparent Mn^{2+}-binding site in MnP from *P. chrysosporium.* In addition to the three amino acid ligands, the hexacoordinate enzyme-bound Mn^{2+} is ligated to the carboxylate of heme propionate 6 and two water molecules, one of which is H-bonded to heme propionate 7 (*23*). An additional residue, R177, which forms a salt bridge with E35, was also recently shown to affect Mn^{2+} binding (*25*). The enzyme contains two heptacoordinate structural Ca^{2+} ions, one distal and one proximal to the heme, which are believed to provide thermal stability to the enzyme (Figure 1) (*26*, *27*).

Other than the unique Mn^{2+}-binding site, the heme environment in MnP appears to be similar to those in other

† This work was supported by Grants MCB-9808430 from the National Science Foundation (to M.H.G.), GM18865 from the National Institutes of Health (to T.M.L.), and BIR-9216592 for the shared Raman spectroscopy instrumentation at OGI (T.M.L.).

* To whom correspondence should be addressed at the Department of Biochemistry and Molecular Biology, Oregon Graduate Institute of Science and Technology, 20000 N.W. Walker Rd., Beaverton, OR 97006-8921. Telephone 503-748-1076; Fax 503-748-1464; e-mail mgold@bmb.ogi.edu.

[1] Abbreviations: 5c and 6c, penta- and hexacoordinate states of the heme iron; ArP, *Arthromyces ramosus* peroxidase; CcP, cytochrome *c* peroxidase; CiP, *Coprinus cinereus* peroxidase; HRP, horseradish peroxidase; HS and LS, high-spin and low-spin electronic configurations of the heme iron; LiP, lignin peroxidase; LMCT, ligand-to-metal charge transfer; MCD, magnetic circular dichroism; MnP, manganese peroxidase; MnPI, manganese peroxidase compound I; MnPII, manganese peroxidase compound II; RR, resonance Raman.

10.1021/bi000679j CCC: $19.00
Published on Web 07/18/2000

plant and fungal peroxidases (*23, 28*−*31*). All of the catalytic residues, including the distal His and Arg and proximal His and Asp, are conserved in MnP, LiP, cytochrome *c* peroxidase, horseradish peroxidase (HRP), and *Coprinus cinereus* peroxidase (CiP)/*Arthromyces ramosus* peroxidase (ArP) (*2, 28*−*30, 32*−*35*). In addition, MnP has two Phe residues in the heme pocket, F45 and F190, which are conserved in HRP and LiP (*23, 28, 33*−*35*) but are replaced by Trp in cytochrome *c* peroxidase (CcP) and ascorbate peroxidase (*32, 36*) and Leu in CiP/ArP (*29, 30*). Site-directed mutagenesis of F190 (Figure 1) in MnP from *P. chrysosporium* indicates a role for this residue in enzyme stabilization (*37, 38*).

In mutants where the F190 residue had been changed to Ala, Leu, Ile (*37*), or Val (*38*), a high-spin (HS) to low-spin (LS) conversion of the heme iron was noted when the solution pH was raised above 6.5. A similar spin change occurred in wild-type MnP but only when the pH was raised above 8.4 (*37*). Preliminary magnetic circular dichroism (MCD) evidence suggested the formation of bis(histidyl)-coordinated heme iron at high pH in both the wild-type and F190I mutant MnP (*37*). In this paper, we provide additional evidence that, in both the F190I mutant MnP and wild-type MnP, this HS → LS transition is due to formation of a low-spin hexacoordinate (6cLS) bis(histidyl) heme iron complex, rather than a hydroxo-heme species, and that the native high-spin pentacoordinate (5cHS) heme iron is fully restored by the addition of excess calcium to the bis-His protein at high pH.

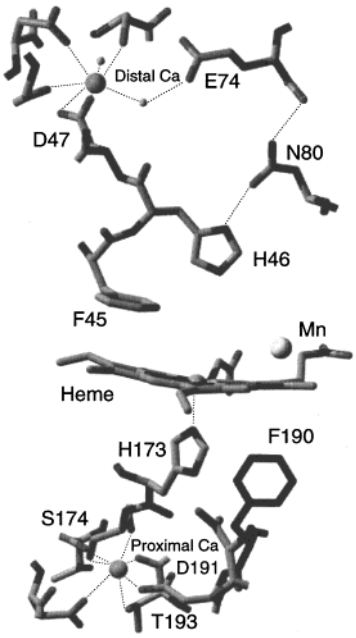

FIGURE 1: Distal and proximal Ca^{2+} binding sites in wild-type MnP from *P. chrysosporium* (*23*). The distal Ca^{2+} is connected to the catalytic distal H46 via the D47 ligand and a hydrogen-bonding network through a water ligand, E74, and N80. The proximal Ca^{2+} is ligated to S174, adjacent to the proximal H173, and D191 and T193, adjacent to F190.

EXPERIMENTAL PROCEDURES

Enzyme Purification. Wild-type MnP was purified from nitrogen-limited shaking cultures of *P. chrysosporium* strain OGC101 as previously described (*15, 39*). The purified protein had an R_z (A_{406}/A_{280}) > 5. The F190I mutant MnP was purified from a transformed strain of *P. chrysosporium*, pAGM5 (*37*), during primary metabolic growth, when endogenous wild-type MnP was not expressed (*25, 37*). Enzyme concentrations were determined from the Soret absorbance ($\epsilon_{406} = 129\ mM^{-1}\ cm^{-1}$) (*15*).

UV−*Visible Spectroscopy.* Electronic absorption spectra of samples containing 100 μM enzyme used in resonance Raman (RR) experiments (Figures 1 and 4) were recorded directly from capillary tubes using a Perkin-Elmer Lambda 9 spectrophotometer. Spectra were obtained before and after laser illumination to monitor sample integrity. Low-pH samples were incubated in water, pH 5.0. High-pH samples were incubated in 50 mM sodium bicine, pH 9.0 (wild type), or 40 mM phosphate, pH 7.5 (F190I). All other electronic absorption spectra were recorded on a Shimadzu UV-260 spectrophotometer with a 1-mL quartz cuvette. Enzymes were reduced by addition of excess dithionite. Solutions were allowed to equilibrate until no further spectral changes occurred (at least 1 min) following addition of components such as dithionite, $CaCl_2$, or buffers to change pH before spectra were recorded. All recorded spectra were stable over the entire time course of experiments (up to 30 min).

RR Spectroscopy. RR spectra were obtained on a custom spectrograph consisting of a McPherson (Chelmsford, MA) model 2061/207 monochromator operated at a focal length of 0.67 m and a Princeton Instruments (Trenton, NJ) LN1100 CCD detector with a Model ST-130 controller. Laser excitation was from a Coherent (Santa Clara, CA) Innova 302 krypton (413.1 nm) laser. The laser line was filtered through an Applied Photophysics (Leatherhead, U.K.) prism monochromator to remove plasma emissions. Incident laser power at the sample was ~15 mW. Spectra were collected in a 90° scattering geometry from solution samples contained in glass capillary tubes at room temperature. Rayleigh scattering was attenuated by the use of a Kaiser Optical (Ann Arbor, MI) super-notch filter. Spectral resolution was set to 4 cm^{-1}. Indene and CCl_4 were used as frequency and polarization standards, respectively.

Chemicals. All chemicals were reagent grade, obtained from Sigma or Aldrich, and used without further purification.

RESULTS

UV−*Vis and RR Spectroscopy of the Oxidized Proteins.* Wild-type MnP exhibits a HS ferric heme absorption spectrum with a Soret maximum at 407 nm and visible band maxima at 502 and 632 nm (*15*). When the pH is raised above 8.4, the spectrum changes to that of a LS ferric heme, as indicated in Figure 2 and Table 1. The Soret peak is red-shifted to 412 nm, becomes less intense, and gains a shoulder at 350 nm; the visible bands at 502 and 632 nm disappear and a new peak is formed at 535 nm. Similar spectral changes also occur in the F190I mutant MnP, though at lower pH (>6.5) (data not shown). The spectra observed are similar to those previously reported for both the F190I mutant and wild-type MnP (*37*) and are provided here as a reference. The alkaline spectra of both proteins resemble the ferric form of the known bis-His heme protein, cytochrome b_5 (Table 1) (*40*). However, the spectra are markedly different than that of alkaline HRP (Table 1) (*40*), strongly suggesting that the alkaline structure is a bis(histidyl) heme complex rather than a hydroxo-heme complex.

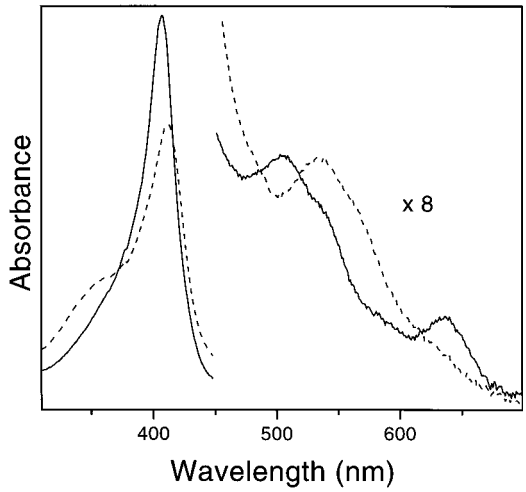

FIGURE 2: Electronic absorption spectra of oxidized (native, ferric) wild-type MnP in distilled water, pH 5.0 (—) and in 50 mM sodium bicine, pH 9.0 (- - -). Spectra are of capillary samples that were used in resonance Raman experiments.

Table 1: Optical Spectral Features of Several Oxidized and Reduced Heme Proteins at Various pH Values

enzyme	pH	electronic absorption maxima (nm)			
ferric wild-type MnP[a,b]	5.0	407	502	530 (sh)	632
	9.0	412	535	559 (sh)	
ferric cytochrome b_5[c]	5.5	413	532	560	
ferric HRP-OH[d]	11.0	416	545	572	
ferrous reduced	5.0	435	515 (sh)	557	586 (sh)
wild-type MnP[a]	9.0	425	529	559	
ferrous F190I MnP[a]	5.0	435	513 (sh)	557	585 (sh)
	9.0	425	529	558	
ferrous cytochrome b_{558}[e]	7.4	426	529	558	

[a] This work. [b] From ref *37*. [c] From ref *40*. [d] From ref *41*. [e] From ref *44*.

To further investigate the nature of the pH-induced HS → LS transition, RR and additional optical spectroscopy were performed. The high-frequency RR spectra for Soret excitation (413.1 nm) characteristic of heme coordination and spin state are shown in Figure 3 and listed in Table 2. The RR spectrum of the wild-type protein at room temperature in distilled water, pH 5.0, is identical to those previously reported in 20 mM succinate, pH 4.5 (*13*), and 20 mM phosphate, pH 6.0 (*21*). The frequencies of the ν_3 modes at 1484 and 1492 cm^{-1} indicate HS species arising from mixed hexa- and pentacoordination in native MnP (*13*, *25*). The F190I mutant MnP displays a similar spectrum in water, pH 5.0 (Figure 3), indicating that the porphyrin core is not affected by the F190I mutation in the proximal domain. At pH 9.0, in 50 mM bicine, HS ν_3 modes for the wild-type MnP disappear with the appearance of a 6cLS ν_3 mode at 1505 cm^{-1} (Figure 3). A concomitant shift of ν_2 from ~1565 to 1580 cm^{-1} and the appearance of a shoulder at ~1638 cm^{-1} from ν_{10} are additional indicators of the pH-induced HS → LS conversion. A similar spectrum is observed in the F190I mutant MnP in 40 mM phosphate, pH 7.5 (Figure 3), indicating that similar LS species are formed in the two proteins, although the transition occurs at lower pH in the mutant enzyme. Both spectra resemble RR spectra of ferric bis(imidazole) heme and ferric cytochrome b_{558} (Table 2) (*42*, *43*). These data strongly suggest that the 6cLS species is formed by a rearrangement at the heme, which allows

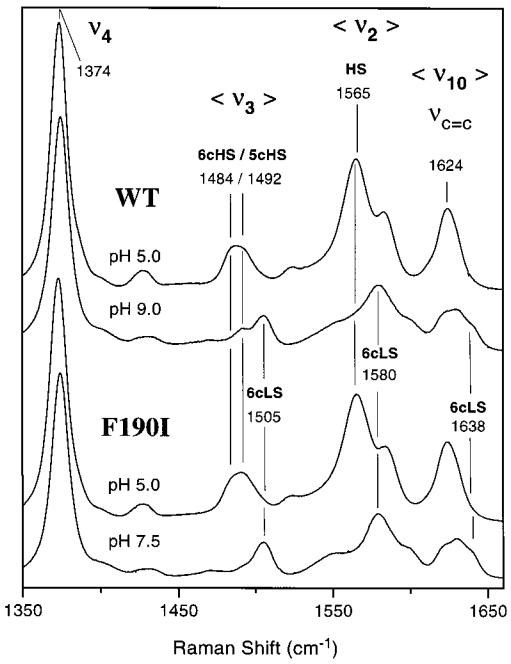

FIGURE 3: High-frequency region of resonance Raman spectra of MnP (~100 μM) at low and high pH obtained with Soret excitation (413 nm) as described. From top to bottom: wild type in distilled water, pH 5.0; wild type in 50 mM sodium bicine, pH 9.0; F190I in distilled water, pH 5.0; and F190I in 40 mM potassium phosphate, pH 7.5. HS, high-spin; LS, low-spin; 5c, pentacoordinate; 6c, hexacoordinate.

Table 2: High-Frequency Resonance Raman Spectral Modes[a]

enzyme	pH	ν_4	ν_3	ν_2	ν_{10}
ferric wild-type MnP[b]	5.0	1374	1484/1492	1565	1624
	9.0	1374	1505	1580	1638
ferric F190I MnP[b]	5.0	1374	1484/1492	1565	1624
	9.0	1374	1505	1580	1638
ferric cytochrome b_{558}[c]		1376	1510	1583	1642
ferric bis(imidazole) heme[d]		1373	1502	1579	1640
ferrous wild-type MnP[b]	5.0	1360	1475	1563	1610
	9.0	1360	1493	1582	1620
ferrous F190I MnP[b]	5.0	1355	1470	1563	1606
	9.0	1359	1493	1582	1626
ferrous cytochrome b_{558}[c]		1360	1490	1585	1610
ferrous bis(imidazole) heme[d]		1359	1493	1584	1617

[a] Frequencies are given in reciprocal centimeters; excitation was at 413.1 nm within the Soret band. [b] This work. [c] From ref *43*. [d] From ref *42*.

coordination of the distal imidazole, H46, resulting in a bis(histidyl) heme iron structure. Low-frequency RR spectra of the wild-type MnP at pH 9.0 in bicine buffer were also recorded (data not shown). No shifts in any bands occurred following incubation of the sample in 75% $H_2{}^{18}O$, consistent with assignment of the LS species as a bis-His coordinated heme iron rather than a hydroxo-iron heme derivative.

Restoration of the Native Structure by Calcium. The ability of calcium to restore the native electronic absorption spectrum in wild-type MnP is demonstrated in Figure 4. The first two spectra are the same in all three panels. Spectrum 1 is of the 5cHS native enzyme in distilled water at pH 5.0, while spectrum 2 is of the 6cLS enzyme formed at pH 8.45 in 50 mM bicine. The same change was also seen upon comparing spectra of the enzyme in 20 mM phosphate at pH 5.0 and 9.0 (data not shown), excluding a buffer effect.

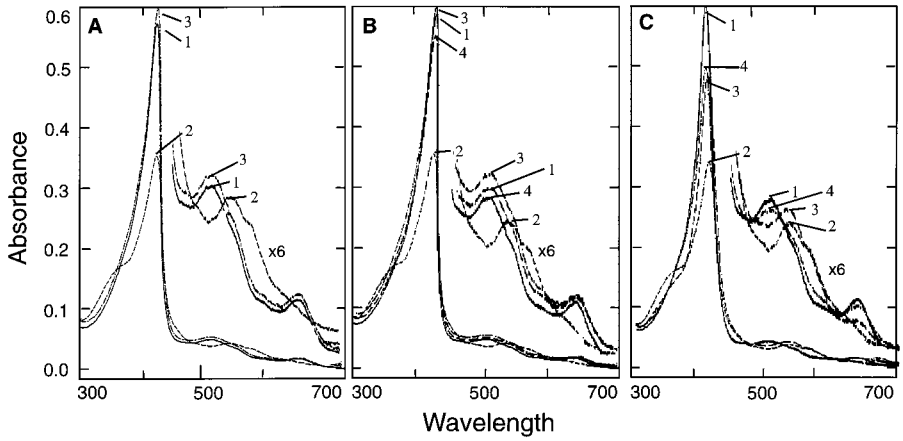

FIGURE 4: Electronic absorption spectra of oxidized (native, ferric) wild-type MnP in distilled water, pH 5.0 (spectrum 1 in all panels) and in 50 mM bicine, pH 8.45 (spectrum 2 in all panels). Addition of 100 mM $CaCl_2$ to the enzyme in water, pH 5.0, does not perturb the spectrum of native MnP (spectrum A3). Addition of 100 mM $CaCl_2$ to the enzyme at pH 8.45 restores the native spectrum at high pH (spectrum B3). Subsequently lowering the solution pH to 5.5 by the addition of 100 mM sodium succinate does not alter the Ca^{2+}-restored spectrum (spectrum B4). First lowering the pH from 8.45 to 5.5 with the addition of 100 mM succinate only partially restores the enzyme (spectrum C3). Subsequent addition of $CaCl_2$ (100 mM) at pH 5.5 (spectrum C4) restores the optical spectrum but does not fully restore the Soret absorption, unlike the addition of $CaCl_2$ at high pH (spectrum B3).

Addition of 100 mM $CaCl_2$ to the native enzyme at pH 5.0 (Figure 4A, spectrum 1) has no effect on the native 5cHS optical spectrum (Figure 4A, spectrum 3). However, addition of calcium to the 6cLS enzyme at pH 8.45 (Figure 4B, spectrum 2) completely restores the native 5cHS spectrum (Figure 4B, spectrum 3). Subsequently lowering the pH of the calcium-restored enzyme by the addition of 100 mM succinate, pH 5.5, does not further alter the HS spectrum (Figure 4B, spectrum 4). In contrast, first lowering the pH from 8.45 (Figure 4C, spectrum 2) to 5.5 without the addition of $CaCl_2$ only partially restores the enzyme (Figure 4C, spectrum 3). The Soret peak is blue-shifted, though less intense, but the visible portion of the spectrum is not restored. Subsequent addition of $CaCl_2$ (Figure 4C, spectrum 4) restores the ligand-to-metal charge transfer (LMCT) bands at 502 and 632 nm but does not completely restore the Soret absorption. Other divalent cations, such as Mn^{2+}, Mg^{2+}, Zn^{2+}, and Cd^{2+}, were incapable of restoring the native spectrum at high pH (data not shown).

UV−Vis and RR Spectroscopy of the Reduced Enzymes. Reduction of the native ferric enzyme with dithionite causes noticeable changes in the electronic absorption spectrum (Figure 5). In distilled water, pH 5.0, the spectrum exhibits maxima at 435, 557, and 586 nm (Table 1), similar to that previously observed in 20 mM succinate, pH 4.5 (*15*). The reduced F190I mutant protein at low pH displays a spectrum nearly identical to that of wild-type MnP (Figure 5, Table 1). At high pH, the spectra of both the reduced wild-type and F190I mutant proteins change (Figure 5). The Soret band at 435 nm is blue-shifted by 10 nm and loses intensity. The peak at 557 is slightly red-shifted, the shoulders at 515 and 585 nm disappear, and a new β band appears at 529 nm. Importantly, the alkaline spectra are very similar to that of ferrous cytochrome b_{558} (Table 1), which is a known 6cLS bis-His heme iron protein (*43, 44*).

RR spectra of the reduced wild-type and F190I mutant MnP proteins at low and high pH are shown in Figure 6. The spectra of both the reduced wild-type and the F190I mutant exhibit ν_3, ν_2, and ν_{10} modes at approximately 1475, 1563, and 1610 cm^{-1}, respectively, indicating ferrous HS

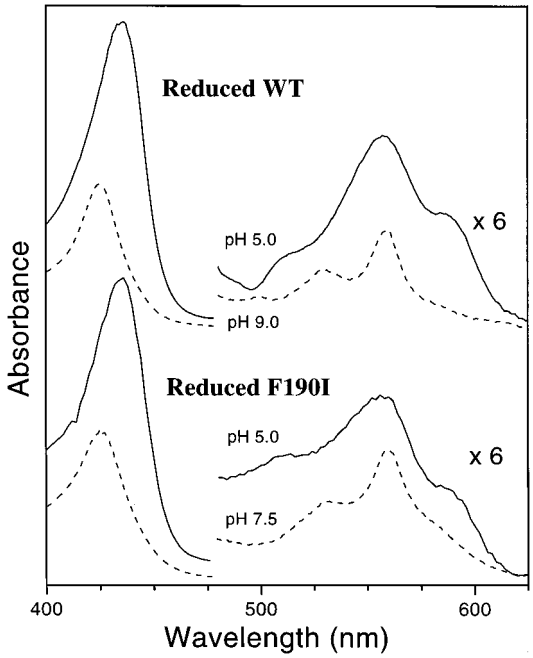

FIGURE 5: Electronic absorption spectra of reduced (ferrous) wild-type MnP and F190I MnP at low pH (—) with both proteins in distilled water, pH 5.0, and at higher pH (- - -) with the wild-type in 50 mM bicine, pH 9.0, and the F190I MnP in 40 mM potassium phosphate, pH 7.5.

species in water at pH 5.0, similar to that previously reported for the wild-type in 20 mM succinate, pH 4.5 (*13*) (Table 2). At higher pH, the reduced wild-type (pH 9.0) and F190I (pH 7.5) enzymes exhibit similar changes in their RR spectra. The HS modes disappear with appearance of LS modes at 1493, 1582, and 1626 cm^{-1}, resulting in spectra similar to those of bis(imidazole) heme and cytochrome b_{558} (Table 2) (*42, 43*).

Restoration of the Reduced Proteins by Calcium. Addition of exogenous Ca^{2+} restored the HS pentacoordinate reduced wild-type structure (Figure 7), similar to results with oxidized proteins. The 5cHS spectrum of reduced wild-type MnP at pH 5.0 is shown in spectrum 1 of Figure 7. The 6cLS species is formed after the pH is raised to 9.0 by addition of 50 mM

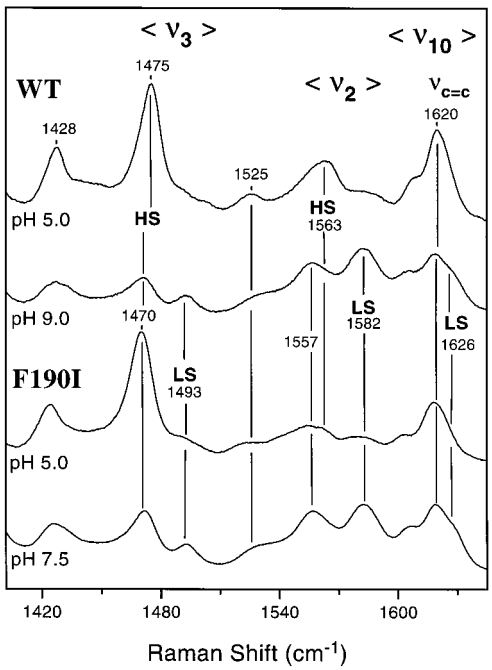

FIGURE 6: High-frequency region of the resonance Raman spectra of reduced MnP under conditions used in Figure 3. From top to bottom: reduced wild type in distilled water, pH 5.0; reduced wild type in 50 mM bicine, pH 9.0; reduced F190I in distilled water, pH 5.0; and reduced F190I in 40 mM potassium phosphate, pH 7.5. HS, high-spin; LS, low-spin.

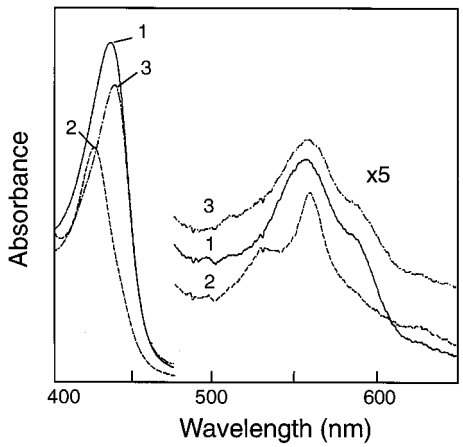

FIGURE 7: Electronic absorption spectra of reduced wild-type MnP in water, pH 5.0 (spectrum 1), or in 50 mM bicine, pH 8.45 (spectrum 2). Addition of 100 mM $CaCl_2$ to the enzyme in spectrum 2, pH 8.45, restores the native spectrum (spectrum 3).

bicine (spectrum 2), while subsequent addition of 100 mM $CaCl_2$ at pH 9.0 restores the 5cHS species (spectrum 3).

DISCUSSION

Electronic absorption spectra of heme proteins are indicators of the HS and LS states of the ferric heme iron. In most plant and fungal peroxidases, the heme iron is coordinated to the protein through the imidazole group of the proximal His residue (*45*−*47*). Primary spectroscopic differences among the various heme proteins result from variations in coordination on the distal side of the iron (*47*). Whereas pentacoordinated heme iron is typically HS, coordination of a sixth ligand results in HS or LS ferric heme species, depending on the ligand field strength of the donor (*48*, *49*). In addition to the Soret band near 405 nm, ferric heme proteins typically exhibit four absorption bands in the visible region of the electronic spectrum. Two LMCT bands near 500 and 630 nm are apparent in spectra of HS derivatives, such as in native MnP, whereas spectra of LS derivatives exhibit the two bands designated α and β near 570 and 540 nm, respectively (*48*). HS → LS transitions frequently occur in peroxidases as the pH is raised. Such "alkaline transitions" appear to involve the ligation of a sixth axial ligand to the pentacoordinate heme iron by either a hydroxyl group, as in HRP (*41*, *50*), or the imidazole of a distal His, as in CcP (*51*).

As previously reported, the electronic absorption spectrum of wild-type MnP indicates an alkaline transition from HS to LS, evidenced by the disappearance of the LMCT bands at 505 and 636 nm and appearance of α and β bands at 559 and 535 nm, respectively, when the pH is raised above 8.4 (Figure 2) (*37*). The resulting spectrum is similar to that of ferric cytochrome b_5 (*40*) (Table 1), a heme protein with bis-His axial coordination of the heme iron. The optical spectrum of the alkaline LS MnP is very different from that of hydroxo-HRP (*41*) (Table 1), supporting the assignment of the LS species in MnP to the formation of a bis-His, rather than a hydroxo-His, coordinated iron. A similar transition occurs in a mutant of MnP where F190 has been replaced by Ile (F190I), Ala (F190A) (*37*), or Val (F190V) (*38*), though at ∼2 pH units lower than for the wild-type MnP. Previous visible MCD spectroscopy of the wild-type and F190I MnP at high pH indicated spectral features similar to those of the imidazole complexes of cytochrome *c* and myoglobin, as well as cytochrome b_5 (*37*, *52*).

Replacement of the proximal residue F190, with Ile, Leu, Tyr, or Ala, does not affect the binding or oxidation of Mn^{2+} (*37*). However, the thermal stability of the protein and the stability of oxidized enzyme intermediates are decreased in the mutant proteins (*37*). The bulky Phe residue may provide a steric barrier that restricts mobility within the heme pocket (*37*). Replacement of the large aromatic ring with smaller hydrophobic residues, such as Ile, may remove these restrictions resulting in increased movement in the heme pocket. This may allow coordination of the distal H46 to the heme iron, thus accounting for the sensitivity of these mutants to external conditions, such as pH.

Upon reduction with dithionite, the electronic spectra of the wild-type and F190I mutant proteins at pH 5.0 display a prominent absorption band at 557 nm with shoulders near 515 and 585 nm (Figure 5), characteristic of pentacoordinate ferrous heme proteins (*53*). When the pH is raised to pH 7.5 for F190I and pH 9.0 for wild-type MnP, the spectra display two prominent absorption bands at 558 and 529 nm, similar to the optical spectrum of ferrous cytochrome b_{558} (Table 1) (*44*), a known bis-His coordinated iron heme protein (*43*, *54*), strongly suggesting the formation of a bis-His heme iron at high pH.

RR spectroscopy is sensitive to the oxidation and spin states of iron porphyrins in proteins. Excitation within the Soret region enhances symmetric modes of vibration within the porphyrin (*55*). The modes ν_3, ν_{10}, and ν_2 are primary RR marker bands that characterize spin state, a measure of the pyrrole nitrogen−carbon stretching frequencies within the porphyrin core that respond to changes in the iron spin (*56*). The RR spectra of the ferric wild-type and F190I mutant MnP are very similar (Figure 3, Table 1), indicating that the

F190I mutation alone does not disturb the porphyrin core. The location of the oxidation state marker band, ν_4, at 1374 cm^{-1} exhibited by both proteins is typical of ferric hemes (*55*). Raising the pH has no effect on the oxidation state of either the wild-type or the F190I MnP (Figure 3). However, shifts in the ν_3, ν_2, and ν_{10} bands at high pH evidence a transition from a predominantly 5cHS species, with a small 6cHS component consistent with aquo-heme, to a fully 6cLS heme iron species (Figure 3). The RR spectra of the alkaline ferric MnPs closely resemble those of ferric cytochrome b_{558} and ferric bis(imidazole) heme (Table 2) (*42, 43, 54*), further supporting the assignment of the 6cLS species to a bis-His axial ligated heme iron.

Incubation of the protein in ^{18}O-labeled water did not result in any changes in the low-frequency spectrum, as would be expected for a hydroxo-ligated heme iron. Other peroxidases, such as HRP and turnip peroxidase, also exhibit HS → LS transitions at high pH that had been previously attributed to coordination of a distal His to the heme iron (*57, 58*). However, more recent studies have shown that incubation of several HRP isozymes in ^{18}O-labeled water at high pH results in shifts in the low-frequency RR spectra (*50*). Bands in the spectra of LS alkaline HRP and turnip peroxidase have since been assigned to Fe−OH stretching at 500−520 cm^{-1}. These peaks are shifted by −9 to −24 cm^{-1} in $H_2{}^{18}O$ (*50*). No corresponding change was detected in the alkaline ferric wild-type MnP, consistent with the assignment of the 6cLS species to a bis-His iron heme rather than a hydroxo-His iron heme complex.

RR spectra of the reduced proteins at high pH (Figure 6, Table 2) also show changes for the ν_3, ν_2, and ν_{10} spin-state modes at high pH for both the wild-type and F190I mutant MnP indicating a HS → LS transition. The RR spectra of the reduced alkaline proteins resemble those of ferrous cytochrome b_{558} and ferrous bis(imidazole) heme (*43, 59*), further supporting the formation of a bis-His species in MnP at high pH.

Together these results provide strong evidence that the 6cLS species formed in both the oxidized and reduced proteins is a bis-His heme iron. It has been proposed that this alkaline 6cLS complex is formed by ligation of the distal H46 to the heme iron as shown for alkaline cytochrome *c* peroxidase (*51*). The identical RR spectra exhibited by the wild-type and F190I mutant proteins indicate that the same heme species is formed by both proteins; however, the F190I mutation allows coordination of the distal His to the heme iron at a lower pH than is observed in the wild-type protein.

The electronic absorption spectrum of the 6cLS MnP formed at high pH is similar to that previously observed in thermally inactivated MnP (*60*). Near IR−MCD spectroscopic analysis suggested the formation of a highly symmetric heme iron in the heat-treated enzyme (*27*). The addition of excess calcium to the thermally inactivated MnP restored the HS native optical spectrum (*27, 60*). Our present results indicate that excess calcium also restores the HS optical (Figure 4) and RR (data not shown) spectra of both wild-type and F190I MnP at high pH. Together, these results indicate that Ca^{2+} mediates the transition from a 6cLS bis-His heme iron back to 5cHS heme iron.

Sutherland and co-workers proposed that loss of the distal Ca^{2+} is responsible for the HS → LS transition upon thermal inactivation (*27, 60*). However, the loss of either or both of the distal or proximal Ca^{2+} ions (Figure 1) could conceivably result in the observed changes. The distal Ca^{2+}-binding site comprises the side chains of D47, S66, and D64, the backbone carbonyls of G62 and D47, as well as two water molecules (Figure 1) (*23*). D47 is on helix B adjacent to the catalytic distal H46, and one of the water ligands to the calcium is bound to E74, which forms part of the H-bond network through Q80 which terminates at the catalytic distal H46 (Figure 1) (ref *23* and references therein). Loss of the distal calcium could result in changes in helix B and/or the E74−N80−H46 H-bond network, which could permit the ligation of the distal H46 to the heme iron.

However, loss of the proximal Ca^{2+} could conceivably result in changes in the conformation of the proximal domain or in the position of the proximal His173, resulting in movement of the heme iron, thus also enabling ligation to the distal H46. The proximal calcium is bound by the backbone carbonyls of T196, S174, and T193 and the side chains of D191, T193, D198, and S174, which is adjacent to the proximal H173 (Figure 1B) (*23*). Indeed, F190 is adjacent to D191 and replacement of F190 may affect stability of the proximal Ca^{2+} binding site. It is therefore conceivable that both Ca^{2+} ions may be involved in preventing/reversing the formation of the bis-His heme complex.

The accessibility of the Ca^{2+} binding site(s) appears to be diminished at low pH. In thermal stability experiments, the addition of exogenous Ca^{2+} was less effective in preventing inactivation of the enzyme at low pH (*60*). Protonation of the carboxyl ligands at the sites may alleviate repulsion in the empty site, resulting in a "collapse" of the site(s) preventing access by Ca^{2+}. The resulting limited access may explain the inability of the cation to completely restore the HS species after the pH was lowered to 5.5 (Figure 4C, spectrum 3). Other cations, such as Mn^{2+} (*39, 60*), also have been observed to confer thermal stability to MnP. Sutherland and co-workers hypothesized that Mn^{2+} stabilized the enzyme by binding at the distal calcium binding site. However, since Mn^{2+} is unable to restore the native HS enzyme at high pH when the site is most exposed, it probably does not bind efficiently at the Ca^{2+} binding site(s). Rather, Mn^{2+} probably confers stability to the enzyme by binding at the Mn^{2+}-binding site. Coordination of a metal at this site, which includes three amino acids and the two heme propionates, may provide additional anchoring of the heme to the protein (*39*).

In conclusion, optical absorption and RR spectroscopy indicate that, at high pH, MnP undergoes a transition from a 5cHS to a 6cLS bis-His iron heme species. No evidence for a hydroxo-heme species was found. Similar LS bis-His species are formed in both the wild-type and F190I mutant MnP proteins, although the pH at which this transition occurs is significantly lower in the F190I MnP variant. The optical spectra of the reduced proteins at high pH closely resemble those of ferrous cytochrome b_{558} (*44*), a known bis-His-ligated protein (*43, 54*). Moreover, the RR spectra of the oxidized and reduced MnP proteins are also similar to those of cytochrome b_{558} and bis(imidazole) heme (*42, 43, 59*). Finally, the 5cHS species is restored upon addition of excess calcium at high pH. This suggests that loss of one or both of the structural Ca^{2+} ions may result in conformational changes that permit coordination of the distal H46 to the heme iron. Other metal cations, including Mg^{2+}, Mn^{2+}, and

Cd^{2+}, were unable to restore the HS pentacoordinate species at high pH.

REFERENCES

1. Hatakka, A. (1994) *FEMS Microbiol. Rev. 13*, 125−135.
2. Gold, M. H., and Alic, M. (1993) *Microbiol. Rev. 57*, 605−622.
3. Gold, M. H., Youngs, H. L., and Sollewijn Gelpke, M. D. (2000) in *Manganese and Its Role in Biological Processes* (Sigel, A., and Sigel, H., Eds.) pp 559−586, Marcel Dekker, New York.
4. Pribnow, D., Mayfield, M. B., Nipper, V. J., Brown, J. A., and Gold, M. H. (1989) *J. Biol. Chem. 264*, 5036−5040.
5. Pease, E. A., Andrawis, A., and Tien, M. (1989) *J. Biol. Chem. 264*, 13531−13535.
6. Godfrey, B. J., Mayfield, M. B., Brown, J. A., and Gold, M. H. (1990) *Gene 93*, 119−124.
7. Mayfield, M. B., Godfrey, B. J., and Gold, M. H. (1994) *Gene 142*, 231−235.
8. Alic, M., Akileswaran, L., and Gold, M. H. (1997) *Biochim. Biophys. Acta 1338*, 1−7.
9. Glenn, J. K., Akileswaran, L., and Gold, M. H. (1986) *Arch. Biochem. Biophys. 251*, 688−696.
10. Harris, R. Z., Wariishi, H., Gold, M. H., and Ortiz de Montellano, P. R. (1991) *J. Biol. Chem. 266*, 8751−8758.
11. Banci, L., Bertini, I., Pease, E. A., Tien, M., and Turano, P. (1992) *Biochemistry 31*, 10009−10017.
12. Dunford, H. B., and Stillman, J. S. (1976) *Coord. Chem. Rev. 19*, 187−251.
13. Mino, Y., Wariishi, H., Blackburn, N. J., Loehr, T. M., and Gold, M. H. (1988) *J. Biol. Chem. 263*, 7029−7036.
14. Wariishi, H., Akileswaran, L., and Gold, M. H. (1988) *Biochemistry 27*, 5365−5370.
15. Glenn, J. K., and Gold, M. H. (1985) *Arch. Biochem. Biophys. 242*, 329−341.
16. Wariishi, H., Valli, K., and Gold, M. H. (1992) *J. Biol. Chem. 267*, 23688−23695.
17. Kuan, I. C., and Tien, M. (1993) *Proc. Natl. Acad. Sci. U.S.A. 90*, 1242−1246.
18. Bao, W., Fukushima, Y., Jensen, K. A., Jr., Moen, M. A., and Hammel, K. E. (1994) *FEBS Lett. 354*, 297−300.
19. Mayfield, M. B., Kishi, K., Alic, M., and Gold, M. H. (1994) *Appl. Environ. Microbiol. 60*, 4303−4309.
20. Kusters-van Someren, M., Kishi, K., Lundell, T., and Gold, M. H. (1995) *Biochemistry 34*, 10620−10627.
21. Kishi, K., Kusters-van Someren, M., Mayfield, M. B., Sun, J., Loehr, T. M., and Gold, M. H. (1996) *Biochemistry 35*, 8986−8994.
22. Whitwam, R. E., Brown, K. R., Musick, M., Natan, M. J., and Tien, M. (1997) *Biochemistry 36*, 9766−9773.
23. Sundaramoorthy, M., Kishi, K., Gold, M. H., and Poulos, T. L. (1994) *J. Biol. Chem. 269*, 32759−32767.
24. Sundaramoorthy, M., Kishi, K., Gold, M. H., and Poulos, T. L. (1997) *J. Biol. Chem. 272*, 17574−17580.
25. Sollewijn Gelpke, M. D., Moënne-Loccoz, P., and Gold, M. H. (1999) *Biochemistry 38*, 11482−11489.
26. Sutherland, G., and Aust, S. (1997) *Biochemistry 36*, 8567−8573.
27. Sutherland, G., Zapanta, L., Tien, M., and Aust, S. (1997) *Biochemistry 36*, 3654−3662.
28. Edwards, S. L., Raag, R., Wariishi, H., Gold, M. H., and Poulos, T. L. (1993) *Proc. Natl. Acad. Sci. U.S.A. 90*, 750−754.
29. Petersen, J. F., Kadziola, A., and Larsen, S. (1994) *FEBS Lett. 339*, 291−296.
30. Kunishima, N., Fukuyama, K., Matsubara, H., Hatanaka, H., Shibano, Y., and Amachi, T. (1994) *J. Mol. Biol. 235*, 331−344.
31. Schuller, D. J., Ban, N., Huystee, R. B., McPherson, A., and Poulos, T. L. (1996) *Structure 4*, 311−321.
32. Finzel, B. C., Poulos, T. L., and Kraut, J. (1984) *J. Biol. Chem. 259*, 13027−13036.
33. Piontek, K., Glumoff, T., and Winterhalter, K. (1993) *FEBS Lett. 315*, 119−124.
34. Poulos, T. L., Edwards, S. L., Wariishi, H., and Gold, M. H. (1993) *J. Biol. Chem. 268*, 4429−4440.
35. Henriksen, A., Schuller, D. J., Meno, K., Welinder, K. G., Smith, A. T., and Gajhede, M. (1998) *Biochemistry 37*, 8054−8060.
36. Patterson, W. R., Poulos, T. L., and Goodin, D. B. (1995) *Biochemistry 34*, 4342−4345.
37. Kishi, K., Hildebrand, D. P., Kusters-van Someren, M., Gettemy, J., Mauk, A. G., and Gold, M. H. (1997) *Biochemistry 36*, 4268−4277.
38. Banci, L., Bertini, I., Capannoli, C., Del Conte, R., and Tien, M. (1999) *Biochemistry 38*, 9617−9625.
39. Youngs, H. L., Sundaramoorthy, M., and Gold, M. H. (2000) *Eur. J. Biochem. 267*, 1761−1769.
40. Strittmatter, P., and Velick, S. F. (1956) *J. Biol. Chem. 221*, 253−264.
41. Keilin, D., and Hartree, E. F. (1951) *Biochem. J. 49*, 88−97.
42. Choi, S., Spiro, T. G., Langry, K. C., Smith, K. M., Budd, D. L., and LaMar, G. N. (1982) *J. Am. Chem. Soc. 104*, 4345−4351.
43. Hurst, J. K., Loehr, T. M., Curnutte, J. T., and Rosen, H. (1991) *J. Biol. Chem. 226*, 1627−1634.
44. Pember, S. O., Heyl, B. L., Kinkade, J. M., Jr., and Lambeth, J. D. (1984) *J. Biol. Chem. 259*, 10590−10595.
45. Ortiz de Montellano, P. R. (1992) *Annu. Rev. Pharmacol. Toxicol. 32*, 89−107.
46. Maranon, M. J. R., and Van Huystee, R. B. (1994) *Phytochem. 37*, 1217−1225.
47. Dunford, H. B. (1999) *Heme Peroxidases*, Wiley-VCH, New York.
48. Palmer, G. (1985) *Biochem. Soc. Trans. 13*, 548−560.
49. Smith, D. W., and Williams, R. J. (1968) *Biochem. J. 110*, 297−301.
50. Sitter, A. J., Shifflett, J. R., and Terner, J. (1988) *J. Biol. Chem. 263*, 13032−13038.
51. Smulevich, G., Miller, M. A., Kraut, J., and Spiro, T. G. (1991) *Biochemistry 30*, 9546−9558.
52. Vickery, L., Nozawa, T., and Sauer, K. (1976) *J. Am. Chem. Soc. 98*, 343−350.
53. Tamura, M., Asakura, T., and Yonetani, T. (1972) *Biochim. Biophys. Acta 268*, 292−304.
54. Fujii, H., Finnegan, M. G., Miki, T., Crouse, B. R., Kakinuma, K., and Johnson, M. K. (1995) *FEBS Lett. 377*, 345−348.
55. Spiro, T. G. (1988) in *Biological Applications of Raman Spectroscopy* (Spiro, T., Ed.) pp 1−38, John Wiley & Sons, New York.
56. Spaulding, L. D., Chang, C. C., Yu, N.-T., and Felton, R. H. (1975) *J. Am. Chem. Soc. 97*, 2517−2525.
57. Morishima, I., Ogawa, S., Inubushi, T., Yonezawa, T., and Iizuka, T. (1977) *Biochemistry 16*, 5109−5115.
58. Teroaka, J., and Kitagawa, T. (1981) *J. Biol. Chem. 256*, 3969−3977.
59. Choi, S., and Spiro, T. G. (1983) *J. Am. Chem. Soc. 105*, 3683−3692.
60. Sutherland, G., and Aust, S. D. (1996) *Arch. Biochem. Biophys. 332*, 128−134.

BI000679J